J Mater Sci (2006) 41:6938–6948
DOI 10.1007/s10853-006-0218-1

Mechanical behavior of cement-based materials reinforced with sisal fibers

H. Jr Savastano · A. Turner · C. Mercer · W. O. Soboyejo

Received: 15 November 2002 / Accepted: 28 October 2003 / Published online: 16 September 2006

Abstract Fiber-reinforced cement composites were produced in Brazil using blast furnace slag cement reinforced with pulped fibers of sisal originated from agricultural by-products. Thin pads were produced by slurring the raw materials in water, followed by de-watering and pressing stages. Studies of mechanical behavior included observations of stable crack growth behavior under monotonic loading (resistance-curve behavior), followed by scanning electron microscopy (SEM) analysis of the fracture surfaces. Reinforcement with cellulose fibers resulted in improved fracture toughness, even after 9 months in laboratory environment. Microscopic analysis indicated a considerable incidence of crack bridging and fiber pull-out in the composite. The shielding contributions from crack bridging are estimated using a fracture mechanics model, before comparing with the measured resistance-curve behavior.

Introduction

In recent years, there have been considerable efforts to develop natural fiber-reinforced cementitious composites for affordable infrastructure [1]. Such composites are typically reinforced with natural fibers obtained from agricultural wastes, such as bamboo fibers [2], sisal fibers [3], sugar cane fibers [4], or fibers extracted from eucalyptus trees [5] or banana pseudo-stem [6]. In most cases, these fibers have little or almost no current economic value [7]. Their use as reinforcements in infrastructural components, such as roof tiles [7], can, therefore, be achieved at relatively low cost. Furthermore, natural fiber-reinforced composites (NFRC) are attractive due to the overall reductions in CO_2 emissions [8], and reduced amounts of energy needed to process natural fiber-reinforced slag-based composites, compared to those of conventional synthetic fiber-cement. They may also be used to replace environmentally hazardous materials, such as asbestos, which are currently used as roof sheet materials in several developing countries [9].

However, the long-term durability of NFRC in potential roof tile applications may be limited by their permeability and resistance to crack growth [10]. These are not properties that can be optimized by the design for improved strength. Instead, a more balanced approach is needed for the optimization of strength, fracture toughness/resistance-curve behavior, fatigue resistance and permeability.

This paper presents the results of a combined experimental and theoretical study of fracture toughness/resistance-curve behavior in a cementitious composite reinforced with sisal fibers. Following a review of related prior work, a brief description of the material processing and microstructure is presented. The resistance-curve behavior of the composite is then described along with the observations of crack/microstructure interactions that control the measured toughening. Subsequently, fracture mechanics models are used to estimate the resistance-curve behavior and the steady-state toughening. The implications

H. Jr Savastano
Rural Construction Group, Faculty of Animal Science and Food Engineering, University of São Paulo, C.P. 23, 13635-900 Pirassununga, SP, Brazil

A. Turner · C. Mercer · W. O. Soboyejo (✉)
Princeton Materials Institute and The Department of Mechanical and Aerospace Engineering, Princeton University, D404 E.-Quad., Olden Street, Princeton, NJ 08544, USA
e-mail: soboyejo@princeton.edu

of the models are then discussed for the design of NFRC with improved crack growth resistance.

Background and related prior work

Background

Natural fibers are widely used as reinforcements in fiber-cement building products [11]. The utilization of plant fibers as reinforcement for cement products falls into two well-defined areas. Firstly, low cost, low performance materials made by labor intensive techniques, and secondly, high performance materials made by conventional fiber cement technology. The Hatschek process (or wet process) [12] is the most widely used method of production. The manufacturing techniques are closely related to conventional heavy paper and board making processes. The formulation of the composite, and hence the cure of the product, varies from country to country, and also from company to company.

In the autoclave process, the matrix is usually a mixture of ordinary Portland cement (OPC) and finely ground silica. In contrast, the more traditional air-cured products require at least 14 days before they can be transported. This air-curing process is lower in capital outlay, but the required formulation involves higher costs. Cement is more expensive than silica and mixtures of organic fibers (mainly PVA—polyvinyl alcohol) and cellulose pulp are necessary to produce air-cured products [11].

In related prior work [13], processing methods have been developed for the fabrication of composites containing blast furnace slag (BFS) based cement reinforced with non-commercial cellulose pulp. This work was motivated by the increasing global commitment to the elimination of chrysotile asbestos. The objective of the prior work was, therefore, the production of non-toxic fiber-cements, for thin roof sheeting applications.

Savastano Jr. et al. [7], John and Zordan [8] and Agopyan and John [14] at the University of São Paulo, Brazil, have focussed on the use of recycled residues in civil construction materials. This group has developed NFRC for potential applications in affordable housing in developing countries. The São Paulo group has also collaborated with the Composites Group of the Forestry and Forest Products (FFP) Division, Commonwealth Scientific and Industrial Research Organization (CSIRO), Australia [6, 13, 15]. This Australian group has optimized the processing parameters for the production of cellulose fiber-reinforced cement composites based on the industrial Hatschek [11].

Shah and Marikunte [16] and Balaguru and Shah [17] have studied the mechanical properties of FRCs in bending. They have also assessed the effects of fiber reinforcement. Their models of load–deflection behavior are based on fracture mechanisms and results from notched beams specimens. Eissa and Batson [18] have used resistance-curve (R-curve) experiments to assess the toughness of high strength steel fiber reinforced concrete notched beams for different fiber types (hooked-end and crimped fibers), and different fiber volume contents (1.0–1.5%). The final a/W values reached ~0.60 (a_0/W ~0.25) and the crack growth resistance (J_R) was over 10^4 J m^{-2} for composites reinforced with 1.5% crimped fibers.

Innovative fiber-cements for cost effective housing

Savastano Jr. et al. [15] have studied the mechanical performance of a clinker free cement-based matrix, reinforced with three different types of vegetable fibers: eucalyptus, banana and sisal. The main raw material of the matrix was a ground BFS, activated by lime and gypsum. The sisal (*Agave sisalana*) field by-product fiber was subjected to the chemi-thermo-mechanical pulping (CTMP) method, based on suggestions by Higgins [19].

Cement composite pads, measuring ~130 × 130 mm, and reinforced with 8% by mass of CTM-pulp, were prepared in the laboratory, using a slurry vacuum de-watering technique. The selection of fiber content was based on the optimum levels found in a similar study published elsewhere [6]. A three-point bend configuration was used in the determination of the modulus of rupture (MOR), modulus of elasticity (MOE) and fracture energy. Fracture energy was calculated by integration of the load–deflection curve to the point corresponding to a reduction in load carrying capacity to 50% of the maximum observed.

After an interval of 28 days from the composite fabrication date, each of the formulations was placed on a rack facing the equator at an angle of inclination of 45°, as specified by ASTM G7-97 [20]. This was done to age them naturally for two years in the temperate environment of Melbourne, Victoria, Australia (37°49′ S of latitude). A corresponding series of composites was exposed in a similar manner to the tropical environment of rural Pirassununga, São Paulo State, Brazil (21°59′ S of latitude). The details are described by Savastano Jr. et al. [15].

Non-aged composites had flexural strengths in excess of 18 MPa, representing a 120% improvement over a plain BFS matrix of similar formulation. As shown in Fig. 1a, 2 years of external exposure to tropical or temperate weather resulted in a considerable reduction in strength, which had fallen to about 5 MPa in the case of the 8% sisal CTMP formulation exposed in Brazil. The loss in mechanical strength of composites subjected to either natural weathering or aging in a controlled environment is attributable to matrix carbonation. Such a mechanism [21,

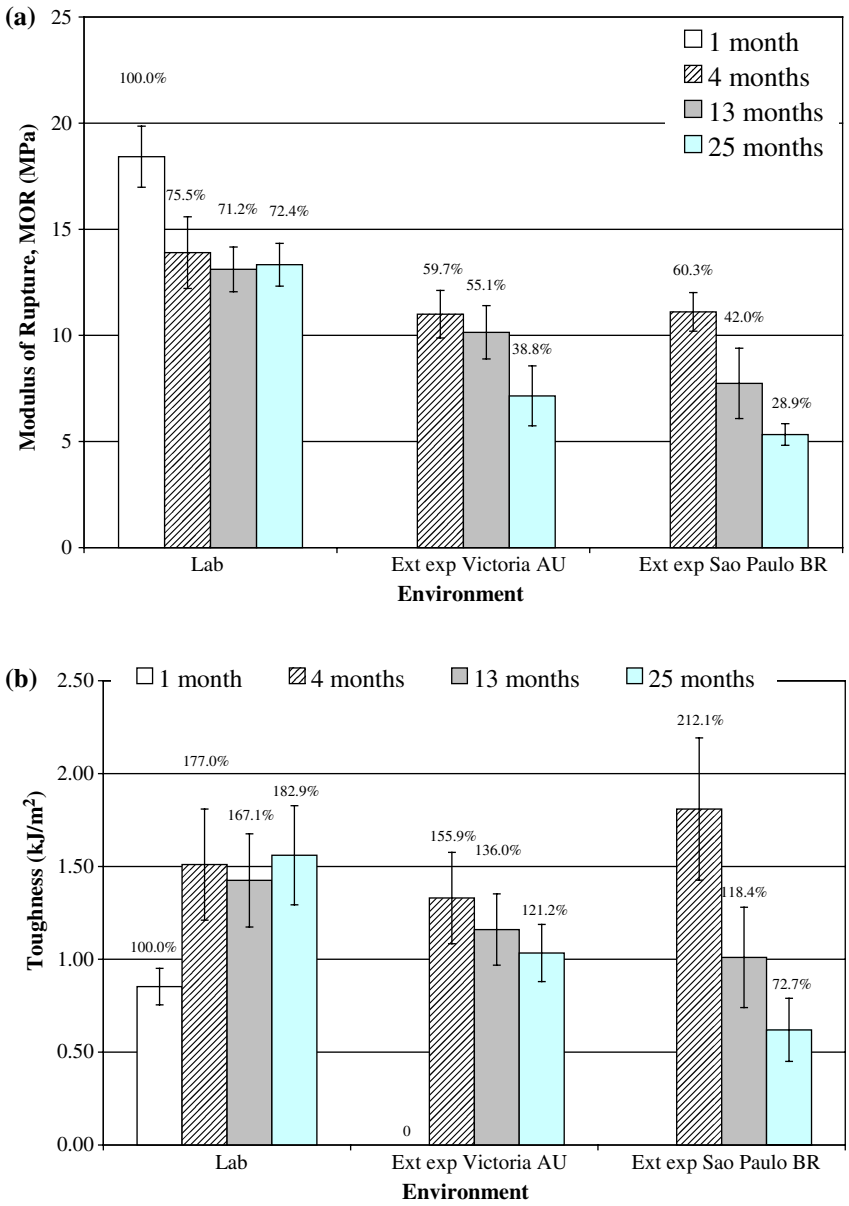

Fig. 1 Sisal CTMP in BFS. Variation in composite mechanical behavior with age and exposition. Error bars indicate single standard deviations of the means. (**a**) MOR. (**b**) Toughness

22], consumes calcium ions from hydration products in combination with the CO_2 present in the atmosphere to form $CaCO_3$, and hence causes the weakening of composites.

Qualitative evaluation using an indicator solution of 2% phenolphthalein in anhydrous ethanol revealed that the aged composites based on clinker-free matrix were completely carbonated. In the case of specimens kept in the laboratory, the ductile behavior of composites signals that the fibers are not being destroyed. This can be understood by the lower alkalinity of pore water of the matrix after carbonation. The high alkalinity of conventional cement-based material (pH ~13) causes the hydrolysis of cellulose chains and/or the dissolution of amorphous constituents of the fiber [23]. The greater severity of the natural environment on composite properties can be connected to matrix leaching, and also to interfacial damage resulting from volume changes of the porous and hygroscopic vegetable fibers inside the cement matrix [24].

Non-aged BFS based composites possessed MOE values of approximately 6 GPa. These are approximately 50% of that of the plain BFS matrix [15]. The reduction is associated with the low modulus of the cellulose fibers employed, and the additional porosity resulting from their inclusion. In the case of sisal CTMP in BFS, the MOE dropped to ~2.1–4.7 GPa, after 25 months of aging. Also, the composite ductilities generally degraded with weathering

and aging. However, improved ductilities were observed in selected composites (Fig. 1b).

The toughness is the matrix property most often enhanced by the presence of fibers (Fig. 1b). For the purpose of this piece of work, the toughness was measured as the fracture energy divided by specimen width and depth at the failure location. The plain matrix presented toughness values between 0.03 and 0.04 kJ/m^2 [13]. The use of 8% sisal fiber content in BFS, followed by exposure in both external environments, resulted in a toughness of at least 0.6 kJ/m^2. Figure 2 depicts an example of load–deflection curves related to specimens after exposition to the action of tropical weather in Brazil. There was a clear decrease in the mechanical behavior up to 25 months of age. In the laboratory environment, the improvements in toughness (area under the stress–strain curve) are associated with increased ductility and reduced overall strength levels. This suggests a compromise between strength and ductility in such composites.

In a previous study of sisal, malva and coir strands with length between 15 and 30 mm in OPC, Savastano Jr. and Agopyan [24] reported reductions in ductility of at least 50% after only 6 months in a laboratory environment. Tolêdo Filho et al. [25] and Bentur and Akers [26] noted similar embrittlement in aged vegetable fiber-OPC composites and found that it could be directly attributed to the petrifaction of the reinforcement, through the migration of hydration products to the fiber lumens and pores.

Material and composite processing

Material

Granulated BFS was provided by Companhia Siderúrgica Tubarão (CST), Brazil, as a by-product of pig-iron manufacture, and characterized by Oliveira et al. [27]. The BFS was ground to an average Blaine fineness of approximately 800 m^2/kg and employed as the main component of a clinker-free binder. Ground gypsum and construction grade hydrated lime are added as activators in proportions of 0.88:0.10:0.02 (BFS:gypsum:lime) by mass.

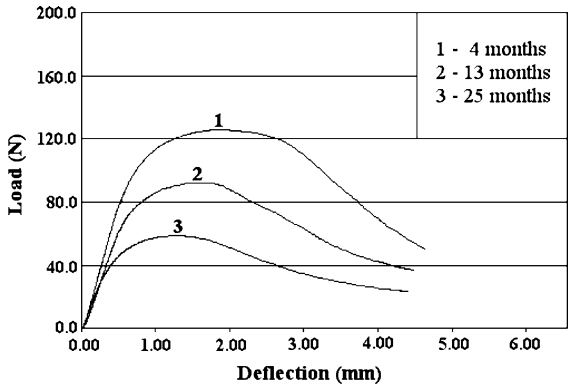

Fig. 2 Load–deflection curves of sisal CTMP in BFS submitted to bending test. Composites exposed to tropical weather and with 4–25 months of age

The sisal (*Agave sisalana*) field by-product is readily available (e.g. 30,000 tones per annum from a producers' co-operative in Brazil) and presently of no commercial value. Utilization of this resource provides a good option for additional income for rural producers. Simple manual cleaning with a rotary sieve provides a suitable starting material. The fibers from sisal strands were subjected to Kraft (or sulfate) pulping, as detailed elsewhere [6], on a laboratory scale at the University of São Paulo (USP), Brazil. After the pulping process, the sisal fiber presented average length and width of, respectively, 1.65 mm and 13.5 μm as previously determined in correlated work [6].

Pulped fibers are preferred for the production of composites using the slurry vacuum de-watering technique, which is a crude simulation in laboratory scale of Hatschek process. During the de-watering stage, the pulp forms a net that is responsible for the retention of cement grains. The small fibers remain homogeneously distributed in two directions (2-D) into the matrix.

Pulping is a deslignification process, which contributes with the stability of vegetable fiber in alkaline environment. The reduction of lignin content should be connected to the better durability of the fiber-cements [23].

Composite processing

Natural fiber reinforced cement composites with fiber mass fractions of 8% (assumed as approximately 10% by volume content) were prepared in the laboratory using a slurry vacuum de-watering technique [5]. Matrix materials were added to the appropriate amount of fiber, already dispersed in water, to form a slurry with approximately 20% of solid materials. After stirring for 5 min the slurry was rapidly transferred to an evacuable ~130 × 130 mm casting box and an initial vacuum (~60 kPa gauge) drawn until the bulk of the excess water was removed, and a solid surface was formed. The moist pad was tamped flat, and the vacuum was re-applied for 2 min.

The pad was then removed from the casting box, transferred to an oiled steel plate and a fine wire mesh (# 1 mm approximately) placed on top. The pad was pressed at 3.2 MPa for 5 min. After pressing, the thickness of the pad was of approximately 15 mm. Upon completion of press consolidation, the plates and meshes were removed and the pads sealed in a plastic bag to cure in saturated air at room temperature for 3 days. The curing was continued for four additional days, with immersion in water at room temperature to optimize the cement hydration. The pads

were then allowed to air cure in a laboratory environment until they were tested, approximately 9 months after production.

Experimental procedures

The resistance-curve experiments were performed on single-edge notched bend (SENB) specimens with thickness (B) of ~7.5 mm, width (W) of ~12.5 mm and length of 65 mm. The initial notch-to-width ratio (a_o/W) was ~0.25 (Fig. 3). The specimens were prepared starting from the raw pads that were produced as described in the previous item (b) Composite Processing. The specimens were prepared by diamond cut off wheel, prior to grinding and final polishing of the specimen sides with diamond grit.

Experiments were conducted under three-point bend loading, with a span of 50 mm. The resistance-curve experiments were performed in an Instron model 8872 servohydraulic testing machine, after pre-cracking under far-field compression [28]. The tests were conducted with the specimens in a laboratory environment with a relative humidity of ~40–50% and a temperature ~25°C.

The specimens were loaded monotonically in incremental stages that corresponded to a stress–intensity-factor range (K) increase rate of 0.05 MPa $\sqrt{m}$. This was achieved at a ramp rate of 2 N s^{-1}. The specimens were then unloaded to examine their sides for evidence of possible crack growth. This was continued until crack growth was detected in an ex-situ optical microscope. Subsequently, the above process was continued, in an effort to study the crack/microstructure interactions that give rise to resistance-curve behavior. This was continued until unstable crack growth/fracture occurred during incremental loading. The calculations of K were obtained from an expression in the ASTM E399-90 code [29]. This gives:

$$K = \frac{PSf\left(\frac{a}{W}\right)}{BW^{1.5}} \tag{1}$$

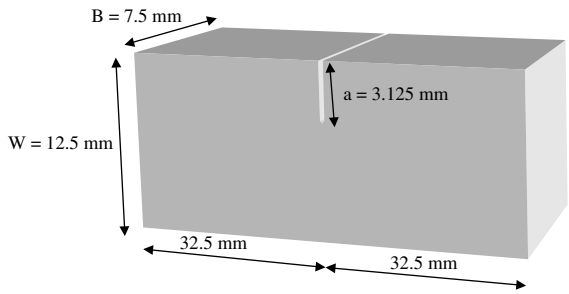

Fig. 3 Schematic representation of the single-edge notched bend (SENB) specimen

where:

$$f\left(\frac{a}{W}\right) = \frac{3\left(\frac{a}{W}\right)^{0.5}\left[1.99 - \left(\frac{a}{W}\right)\left(1 - \frac{a}{W}\right)\left(2.15 - 3.93\frac{a}{W} + 2.7\frac{a^2}{W^2}\right)\right]}{2\left(1 + 2\frac{a}{W}\right)\left(1 - \frac{a}{W}\right)^{1.5}} \tag{2}$$

P is the applied load, B is the specimen thickness, W is the specimen depth (width), S is the span, and a is the crack length. The function $f(a/W)$ is a geometry/compliance function.

After specimen fracture, the fracture modes were investigated using a field emission gun (FEG) scanning electron microscope (SEM), operating at an accelerating voltage of 10 kV, using secondary electron (SE) or backscattered electron (BSE) imaging modes.

Micromechanical modeling

Since crack bridging was commonly observed in this work, it is of interest to analyze its role during crack growth under monotonic loading. An energy approach [30] may be used to explain the toughening due to crack bridging by ductile fibers or ligaments. The toughening of the brittle matrix due to small-scale bridging (SSB) by ductile fiber reinforcement may be idealized using an elastic–plastic spring model (Fig. 4), as proposed by Budiansky et al. [31], and Li and Soboyejo [32]. For SSB, in which the size of the bridging zone is much smaller than the crack length [33], the extent of ductile phase toughening may be expressed in terms of the maximum stress intensity factor the material can sustain before failure (fracture toughness). Hence, the fracture toughness of the composite, K_c, can be expressed as the sum of the matrix fracture toughness, K_m, and the toughening component due to crack bridging, ΔK_{ssb}. The fracture toughness of the ductile-reinforced composites may thus be estimated from Eq. 3, as stated by Soboyejo [30]:

$$K_c = K_m + \Delta K_{ssb} = K_m + \left(\frac{2}{\pi}\right)^{0.5} \alpha V_f \int_0^L \frac{\sigma_y}{x^{0.5}} dx \tag{3}$$

where α is the constraint/triaxiality factor (typically between 1 and 3) [33, 34], V_f is the volume fraction of ductile phase, L is the length of the bridging ligament, σ_y is the uniaxial yield stress, and x is the distance from the crack tip (Fig. 4a).

For large-scale bridging (LSB) conditions (where the length of the bridging zone is comparable to the overall

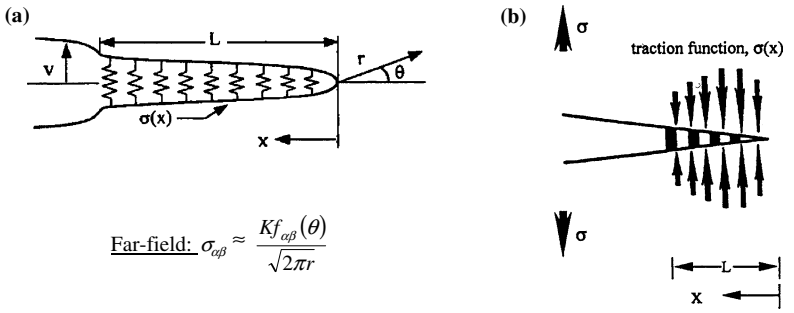

Fig. 4 Schematic illustrations of crack bridging. (**a**) Spring model. (**b**) Weighted distribution of tractions across ligaments

crack size), the toughening increment (ΔK_{lsb}) is given by Eq. 4 [32–36].

$$\Delta K_{\mathrm{lsb}} = V_{\mathrm{f}} \int_{L} \alpha \sigma_y h(a,x) \mathrm{d}x \tag{4}$$

where $h(a, x)$ is the weighting function for the bridging tractions (Fig. 4b) [37]. This is given by Fett and Munz [37] to be:

$$h(a,x) = \sqrt{\frac{2}{\pi a}} \frac{1}{\sqrt{1-\frac{x}{a}}} \left(1 + \sum_{(v,\mu)} \frac{A_{v\mu}\left(\frac{a}{W}\right)}{\left(1-\frac{a}{W}\right)} \left(1-\frac{x}{a}\right)^{v+1} \right) \tag{5}$$

where the coefficients ($A_{v\mu}$) are given in Table 1 for a single edge notched bend (SENB) specimen.

Results and discussion

Resistance-curve behavior

The resistance-curve obtained for the fiber–cement composite is shown in Fig. 5. Stable crack growth initiated at a stress intensity factor, K_0, of ~0.7 MPa $\sqrt{m}$. The amount of stable crack growth (Δa) was considered around 1.8 mm (a/W ~0.4), and the stress intensity factor reached ~1.0 MPa $\sqrt{m}$.

Three repetitions were carried out in the present study. Some experimental results reached stable crack growth (Δa) of 2.4 mm, corresponding to K = 1.5 MPa $\sqrt{m}$ and a/W ~0.44. Such a different trend was not considered as representative of the intrinsic behavior of the composite but as the influence of the specimen dimensions, when the crack growth was too close to the specimen width. Visalvanish and Naaman [38] have reviewed existing studies on fracture of cement-based materials and discussed the end dominant zone of the specimen with a similar behavior. As the crack reaches the end of the specimen, bending stress over the end portion becomes dominant. The stress intensity factor can then be determined from the relation given by Paris and Sih *apud* Visalvanish and Naaman [38] as expressed in the Eq. 6. The application of the Paris and Sih method gave a good agreement with the experimental data for the higher values of Δa as showed in the Fig. 5.

$$K = \frac{P(2.71W + 1.63a)}{B(W-a)^{1.5}} \tag{6}$$

Table 1 Summary of Fett and Munz [37] parameters for SENB specimen subjected to weighted crack bridging fractions

N	μ				
	0	1	2	3	4
0	0.4980	2.4463	0.0700	1.3187	–3.067
1	0.5416	–5.0806	24.3447	–32.7208	18.1214
2	–0.19277	2.55863	–12.6415	19.7630	–10.986

The presence of short vegetable fibers has a significant effect on the fracture toughness, and on the extent of stable crack growth observed in this cement-based material. The mechanical behavior of the composite could be even more favorable by the use of hybrid reinforcement of cellulose pulp combined with discontinuous fibers of non-pulped sisal for example. Studies carried out by Castro and Naaman [39] indicated that good mechanical results could be achieved by cement-based mortars reinforced with *Agave* fibers up to 75 mm long under normal environmental exposures. The authors also informed that the utilization of long fibers with volume fraction from 5 to 11% prevented erratic results, the analysis being simplified with less variability. With longer fibers, the crack length and the bridging zone are expected to become very proximate for a reasonable size composite.

It is of interest to compare the results of the current study to prior reports of fracture toughness/resistance-curve behavior in cementitious materials. In the present work, the random distribution of short fibers makes the modeling of crack bridging more challenging. Similar resistance-curve

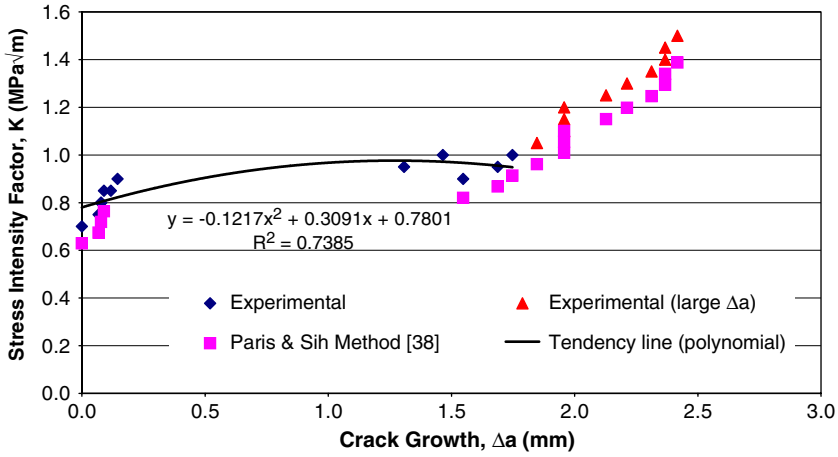

Fig. 5 Experimentally measured Resistance-curve (*R*-curve) behavior of the sisal fiber-reinforced cement composite

behavior was observed in cement matrices reinforced with different types of fibers, such as carbon, steel and polypropylene, in studies by Eissa and Batson [18] and by Banthia and Sheng [40]. Banthia and Sheng [40] used the *R*-curve experiment to study the effects of polypropylene fibers (4 μm diameter, 6 mm long, E = 1.41 GPa, tensile strength = 32 MPa) as reinforcements in a cement paste based matrix. Following reinforcement with up to 3% by volume of fiber content, the improvement of the composite toughness was significant, compared with the un-reinforced matrix. At this level of reinforcement, the effective final crack length, a_{eff}, (measured using compliance method) varied from 8 to 8.45 mm (W ~25 mm) and values for K_{I} reached ~0.55 MPa $\sqrt{m}$. Ouyang and Shah [41] and Visalvanich and Naaman [38] proposed values of 0.8 and 1.3 MPa $\sqrt{m}$, respectively, for the critical stress intensity factor (K_{Ic}) for plain cement mortars.

Fracture modes

Figure 6a and b show representative images of the fracture surface of the composite at low and high magnification, respectively. There is a considerable incidence of pulled-out fibers and some voids left by pulled-out fibers that remained attached to the opposite fracture surface. In contrast, Bentur and Akers [26] suggested that brittle fracture of fibers could be expected in air-cured OPC-based composites after aging. In the present work, the fibers seem to be largely intact after 9 months under laboratory environment.

Savastano Jr. et al. [15] reported a high incidence of fiber pullout in BFS-based composites reinforced with pulp from banana or sisal plants, after 12 months under natural weathering. In that study, such behavior was related to higher toughness of the aged composites, in comparison with the corresponding non-aged material. The increased toughness was associated largely with reduced strength and increased ductility levels, resulting ultimately in greater energy dissipation prior to final fracture. The increased ductility was attributed mainly to crack bridging and fiber pull-out.

Figure 6c–e shows evidence of considerable interactions between the matrix and sisal fibers, as can be noted from the effective matrix/fiber bond in Fig. 6c (as indicated by the arrow), matrix incrustation in the surface of filaments (Fig. 6d) and pulled-out fibers with fractured tips in Fig. 6e. This suggests significant energy dissipation in the interfacial zone during fracture. Figure 6f shows a bunch of individual fibers, suggesting that the pulping process was incomplete. In spite of this, it is important to note that the composite exhibits reasonable resistance-curve behavior according to related studies [18, 38, 40, 41]. This suggests that the pulp quality does not need to be equivalent to that required by the paper industry [6].

Comparison of bridging predictions with experimental results

The measured resistance-curve behavior in Fig. 5 can be compared with the predicted based on the micromechanical models presented earlier in Sect. 4. As in previous work [34], SSB was presumed to occur for crack growth, Δa, less than ~0.5 mm, and LSB was assumed for $\Delta a \geq 0.5$ mm. Hence, the predictions of the initial portion of Fig. 5 were based on Eq. 3, while the predictions of toughening in the LSB-regime were based on Eq. 4. Typical values of crack bridging parameters such as bridge length, L, and fiber volume fractions were extracted by quantitative image analyses of side profiles, shown in Fig. 7a and b.

Using the measured initiation toughness, K_0, of ~0.7 MPa $\sqrt{m}$, the K levels corresponding to each increment of crack growth can be estimated from the sum of K_i and the toughening increment due to crack bridging, ΔK_{b}. The resistance-curve is, therefore, given simply by

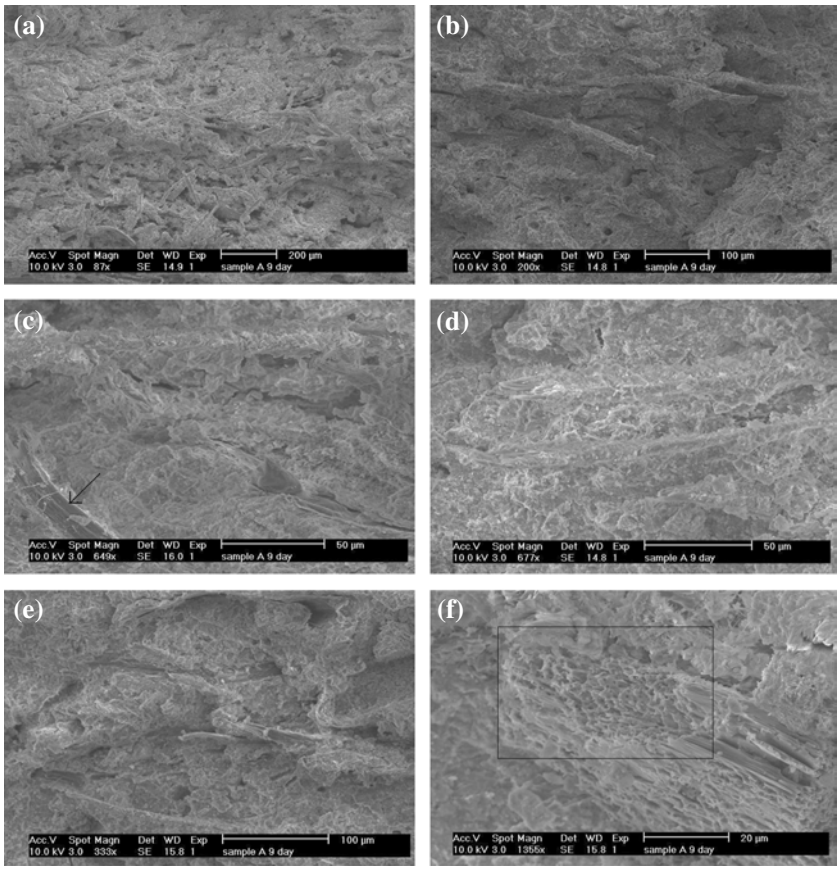

Fig. 6 SEM image of the fractured surface of sisal fiber–cement. (**a**) General view. (**b**) Detail of pulled-out fibers. (**c**) Fiber–matrix interfacial zone (the arrow indicates the good adhesion at the interface). (**d**) Fibers with matrix material incrusted in their surface. (**e**) Fibers partially pulled-out with fractured tips. (**f**) Bunch of individual fibers as a consequence of incomplete pulping (the rectangular frame highlights the tip of the bunch of fibers)

$K_0 + \Delta K_{ssb}$ for SSB and $K_0 + \Delta K_{lsb}$ for LSB. In the case of SSB, the constraint/triaxiality factor was assumed to be ~1, and the value of V_f was estimated to be 0.25 based in quantitative analyses of Fig. 7. The fiber tractions were assumed to correspond to ~6 MPa, which corresponds roughly to the lower level of natural fibers strengths [42]. This is consistent with prior work [15], in which, the composite strengths were found to be reduced by about half, after 1 year of interactions between the natural fibers and the cement matrix.

The predictions for SSB are compared with the measured resistance-curve in Fig. 8. The value reached for the overall increment, $\Delta K_{ssb} = 0.136$ MPa $\sqrt{m}$, is an underestimation of the experimental measurements. This behavior is in agreement with a previous work by Kung et al. [33] regarding the predicted resistance-curve.

For the LSB prediction, the values for α, V_f, σ_y and L were adopted to be as those used for the SSB predictions. A comparison of the predictions obtained from Eq. 4 and the measured LSB resistance-curve is also presented in Fig. 8. The experimental values of stable crack growth (Δa) were considered around 1.5 mm and 1.8 mm, and the stress intensity factor reached ~1.0 MPa $\sqrt{m}$. The LSB model also predicts the overall trends as an underestimation (~0.9 MPa $\sqrt{m}$) although much closer of the experimental data.

The resistance-curves are specimen dependent. Hence, different resistance-curves would be expected from different specimens due to differences in the heterogeneous microstructures. The measured toughness levels are also dependent on crack length. It is, therefore, important to obtain estimates of fracture toughness that do not depend so strongly on crack length or specimen geometry. The estimates would represent the true intrinsic toughness of the composites, which would normally require the testing of very large specimens. Such estimates of the intrinsic composite fracture toughness can be obtained by simulating the possible effects of LSB on the weight function, $h(a, x)$, in Eqs. 4 and 5. This can be achieved by artificially increasing the specimen width, W, such that $W \to \infty$. The function $h(a, x)$ is found to approach an asymptotic value when this is done (Fig. 8).

The resulting value of ΔK_{lsb} corresponding to the above asymptotic value is ~0.09 MPa $\sqrt{m}$. From Eq. 4, this gives an estimated intrinsic fracture toughness value of ~0.84 MPa $\sqrt{m}$. The maximum K in the R-curve is around 1.0 MPa $\sqrt{m}$. The difference between the simulations with real value of W (large scale bridging model) and with $W \to \infty$ (intrinsic toughness) shows the influence of the specimen dimensions especially for higher values of Δa (Fig. 8).

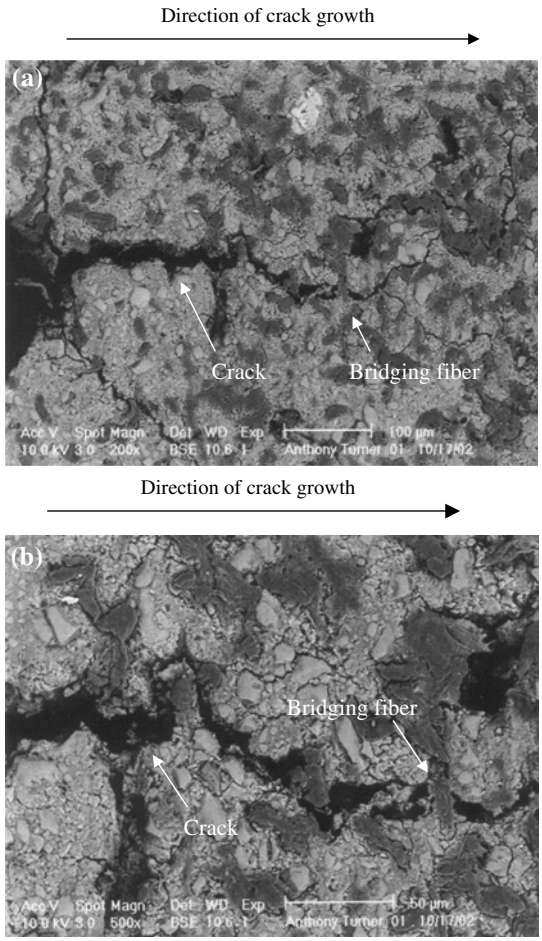

Fig. 7 Backscattering electron image (BSEI) of the sample surface. (**a**) Notch end (left) showing cracks and composite bridges. Fibers are seen in dark gray. (**b**) Higher magnification to highlight the composite bridges

Scale effects are very important for cement composites. Balaguru and Shah [17] reported that first-cracking strength decreases with increase in beam size. It is recognized that reasonably larger scale tests would be able to give an idea of the true mechanical behavior.

Although both SSB and LSB models capture the general trends of the measured resistance-curves, the values predicted by the models are lower than the corresponding experimental measurements. This may be connected to the in-homogeneity of the material, the random distribution of the reinforcement and the degradation of ligaments bridges between the cement matrix and the natural fibers.

The considerable variability of mechanical results of the NFRC is understandable by the method of fabrication and properties of untreated vegetable fiber. Gatto et al. [43] applied the same experimental procedure for fiber–cement production, which was associated to poor physical behavior (water absorption of 25% by mass, bulk density of 1.5 g/cm^3 and permeable void volume of approximately 40%) for similar composites produced with BFS matrix reinforced with sisal kraft pulp. Such characteristics of the material could limit the usefulness of rather sophisticated experimental and analysis techniques used in the experimental program. In spite of these limitations, the above work has significant implications for the design of durable natural fiber-reinforced cement-based composites. First, the measured resistance-curves suggest that use of lower cost sisal fibers promotes toughening behavior that is comparable to that of synthetic fiber-reinforced composites. Furthermore, since the general trends in the measured resistance-curves can be predicted, the current work suggests that the small- and the LSB models can be used to guide the development of NFRC that are more resistant to crack growth. For example, both the SSB and the LSB models suggest that improved fracture toughness/resistance-curve behavior can be engineered by increasing the fiber strength, bridge length and fiber volume fraction. However, increased fiber strength and volume fraction

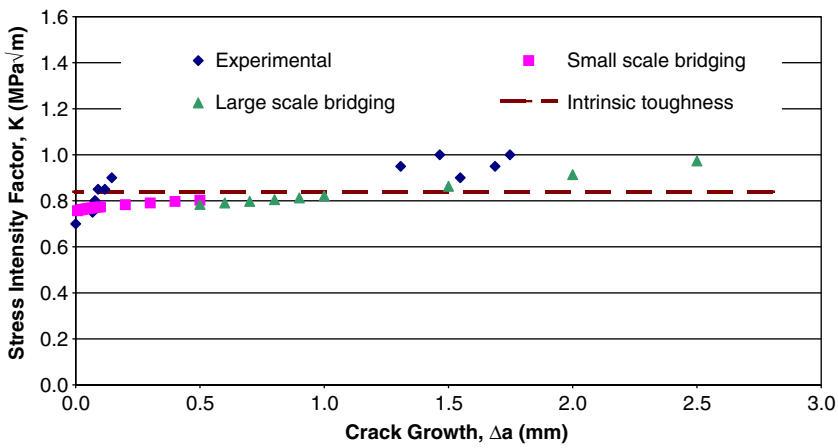

Fig. 8 Comparison of measured and calculated resistance-curves using small and large scale bridging models for the sisal fiber-reinforced cement composite

must be designed judiciously, since these may also promote premature fiber fracture prior to the development of significant bridging zone.

Since the initial fiber strengths are degraded significantly by cement/fiber interactions [24, 44], this suggests that the use of fiber coatings may be the key to the engineering of improved NFRC that are more resistant to fracture/cracking. Such coatings may also serve multifunctional roles by providing increased resistance to water uptake and environmentally induced damage. The development of coatings or surface treatments for NFRC is clearly the challenge for future work. Another possibility could be the modification of the cement matrix aiming to be less aggressive to the fiber by the use of pozzolanic or slag additions or by the use of polymer modified cement systems [15, 42]. Additionally the production of composites with lower permeable porosity could also contribute to the better mechanical performance, to the less variability in the results and to the better durability under normal environment [42]. Such studies are intrinsically associated with the viable utilization of natural fiber cement-based materials for the production of thin panels in cost effective building applications.

Summary and concluding remarks

1. Cement paste based on BFS and reinforced with sisal Kraft pulp has an initiation and a final propagation toughness of ~0.7 MPa $\sqrt{m}$ and 1.0 MPa $\sqrt{m}$, respectively. This toughness is considered acceptable for production of thin panels for internal uses [15].
2. Fractographic analysis confirmed a satisfactory interaction between the cement matrix and the fiber reinforcement in this ongoing work. After 9 months in a closed environment, the fracture surface of the failed *R*-curve specimens exhibited a high incidence of pulled-out fibers. Crack bridging and filament fracture were also observed after some debonding. The fracture modes, therefore, suggest high-energy absorption during the *R*-curve tests.
3. The toughness values predicted by both small and large scale bridging models were lower than the corresponding experimental measurements, since these models are not able to account for all the variables involved in toughening mechanisms during fracture of these composite materials. The LSB model yielded more accurate toughness predictions at large crack lengths.
4. The intrinsic toughness was estimated to be ~0.84 MPa $\sqrt{m}$. This represents the true specimen-independent fracture toughness value of the material that was examined in this study.

Acknowledgments The research is supported by the Materials Division of the National Science Foundation (Grant Number DMR 0231418 and DMR 0303492). The authors are grateful to Dr. Carmen Huber of NSF for her encouragement. The authors would also like to thank Mr. Victor Odunsi for his support. Appreciation is extended to Dr. Marie Ange Arsène and to Mr. Jun Lou for useful discussions, and their help on the bridging models. The first author also express his gratitude to the National Council for Scientific and Technological Development (CNPq) and the Co-ordination for the Improvement of Higher Education Personnel (Capes) for their support, and to Mr. Leandro Cunha and Mr. Paulo Silva for their skilful assistance at the Laboratory of Rural Construction of University of São Paulo, Brazil. Finally, the authors would like to thank Dr. Seyed Allameh for assistance with scanning electron microscopy techniques.

References

1. Swamy RN (ed) (1988) Natural fibre reinforced cement and concrete. Blackie, Glasgow
2. Coutts RSP, Ni Y (1995) Cem Concr Compos 17:99
3. Savastano H Jr, Warden PG, Coutts RSP (2003) Cem Concr Compos 25:311
4. Bilba K, Arsene M-A, Ouensanga A (2003) Cem Concr Compos 25:91
5. Eusebio DA, Cabangon RJ, Warden PG, Coutts RSP (1998) In: Hadi YS (ed) Proceedings of the 4th Pacific Rim Bio-Based Composites Symposium, Bogor, November 1998, Bogor Agricultural University, Bogor, p 428
6. Savastano H Jr, Warden PG, Coutts RSP (2000) Cem Concr Compos 22:379
7. Savastano H Jr, Agopyan V, Nolasco AM, Pimentel L (1999) Constr Build Mater 13:433
8. John VM, Zordan SE (2001) Waste Manage 21:213
9. Heinricks H, Berkenkamp R, Lempfer K, Ferchland H-J (2000) In: Moslemi AA (ed) Proceedings of the 7th International inorganic-bonded wood and fiber composite materials conference, Sun Valley, September 2000, University of Idaho, Moscow, 2000, 12 p (Siempelkamp Handling Systems report)
10. Savastano H, Jr, Agopyan V, John VM (2000) In: John VM, Agopyan V (eds) Proceedings of the CIB Symposium on construction & environment, São Paulo, November 2000, CIB-Escola Politécnica da Universidade de São Paulo, São Paulo, 10 p
11. Coutts RSP (1988) In: Natural Fibre Reinforced Cement and Concrete, Blackie, Glasgow, p 1
12. Coutts RSP (1992) In: Swamy RN (ed) Proceedings of the 4th International Symposium on fibre reinforced cement and concrete, Sheffield, July 1992, E & FN Spon, London, p 31
13. Savastano H Jr, Warden PG, Coutts RSP (2001) Cem Concr Compos 23:389
14. Agopyan V, John VM (1992) Build Res Informat 20:233
15. Savastano H Jr, Warden PG, Coutts RSP (2001) In: Duncan J (ed) Proceedings of the CIB world building congress, Wellington, April 2001, Branz, Wellington, 11 p
16. Shah SP and Marikunte SS (1993) In Proceedings of the 1st ACBM annual faculty enhancement workshop, Evanston, July 1993, NSF-ACBM Center, Evanston, ch. 8, p. 226
17. Balaguru PN, Shah SP (1992) Fiber-reinforced cement composites. McGraw-Hill, New York
18. Eissa A-B, Batson G (1996) Cem Concr Compos 18:125
19. Higgins HG (1996) Paper physics in Australia. CSIRO Division of Forestry and Forest Products, Melbourne
20. American Society for Testing and Materials (1997) Standard practice for atmospheric environmental exposure testing of nonmetallic materials G7–97, ASTM, West Conshohocken, Book of Standards v. 14.04, 7 p

21. Wang S-D, Pu X-C, Scrivener KL, Pratt PL (1995) Adv Cem Res 7:93
22. Taylor HFW (1997) Cement chemistry. Thomas Telford, London
23. Gram HE (1988) In: Natural fibre reinforced cement and concrete. Blackie, Glasgow, p 143
24. Savastano H Jr, Agopyan V (1999) Cem Concr Compos 21:49
25. Tolêdo Filho RD, Scrivener K, England GL, Ghavami K (2000) Cem Concr Compos 22:127
26. Bentur A, Akers SAS (1989) Int J Cem Compos Lightweight Concr 11:99
27. Oliveira CTA, John VM, Agopyan V (1999) In: Proceedings of the 2nd international conference on alkaline cements and concretes, Kiev, May 1999, Kiev State Technical University of Construction and Architecture, Kiev, p 18
28. Soboyejo WO, Venkateswara Rao KT, Sastry SML, Ritchie RO (1993) Metall Trans A 24A:585
29. American Society for Testing and Materials (1997) Standard test method for plane-strain fracture toughness of metallic materials E399–90, ASTM, West Conshohocken, Book of Standards v. 03.01, 31 p
30. Soboyejo WO (2002) In: Mechanical properties of engineered materials, Marcel Dekker Publishers, New York, p 414
31. Budiansky B, Amazigo JC, Evans AG (1988) J Mech Phys Solids 36:167
32. Li M, Soboyejo WO (2000) Metall Mater Trans A 31A:1385
33. Kung E, Mercer C, Allameh S, Popoola O, Soboyejo WO (2001) Metall Mater Trans A 32A:1997
34. Lou J, Soboyejo WO (2001) Metall Mater Trans A 32A:325
35. Bloyer DR, Venkateswara Rao KT, Ritchie RO (1998) Metall Mater Trans A 29A:2483
36. Bloyer DR, Venkateswara Rao KT, Ritchie RO, (1999) Metall Mater Trans A 30A:633
37. Fett T, Munz D (1994) Stress intensity factors and weight functions for one-dimensional cracks, Institut fur Materialforschung, Kernforschungszentrum Karlsruhe. Report KfK 5290
38. Visalvanich K, Naaman AE (1981) J Eng Mech Div 107:1155
39. Castro J, Naaman AN (1981) ACI J 78:69
40. Banthia N, Sheng J (1996) Cem Concr Compos 18:251
41. Ouyang C, Shah SP (1992) Cem Concr Res 22:1201
42. Beaudoin JJ (1990) Handbook of fiber-reinforced concrete: principles, properties, developments and applications. Noyes, Park Ridge
43. Gatto EG, Kawabata CY, Savastano H Jr, (2003) J Braz Soc Agric Eng 23:211 (in Portuguese)
44. Tolêdo Filho RD, Ghavami K, England GL, Scrivener K (2003) Cem Concr Compos 25:185